



*Conference Proceedings of the 5th Asia Pacific Luminescence and Electron Spin Resonance Dating Conference
Oct 15th-17th, 2018, Beijing, China*

Guest Editor: Grzegorz Adamiec

ASSESSING THE DATING POTENTIAL OF VIOLET STIMULATED LUMINESCENCE PROTOCOLS

MARIANA SONTAG-GONZÁLEZ^{1,2}, MARINE FROUIN², BO LI^{1,3} and JEAN-LUC SCHWENNINGER²

¹*Centre for Archaeological Science, School of Earth, Atmospheric and Life Sciences, University of Wollongong, Wollongong, NSW 2522, Australia*

²*Research Laboratory for Archaeology and the History of Art, University of Oxford, South Parks Road, Oxford, OX1 3TG, UK*

³*Australian Research Council (ARC) Centre of Excellence for Australian Biodiversity and Heritage, University of Wollongong, Wollongong, NSW 2522, Australia*

Received 14 January 2019

Accepted 12 July 2019

Abstract: Violet stimulation is a new development in optical dating which has been suggested to extend the upper age limit of optically simulated luminescence (OSL) dating of quartz. Despite the reported advantage, few validation tests and applications have been published so far. The present study investigated the violet stimulated luminescence (VSL) using a single aliquot regenerative dose (SAR) protocol and a multiple aliquot additive dose (MAAD) protocol. Sedimentary quartz samples from four archaeological sites in Europe with independent age controls spanning 40–900 ka were used, including Grotte Mandrin (France), Brooksby Quarry (UK), Cueva Negra del Estrecho del Río Quípar (Spain) and Sima de las Palomas del Cabezo Gordo (Spain). The equivalent dose of a relatively young sample (~40 ka) was successfully determined. However, significant underestimations were observed for older samples with higher doses. These findings indicate the need for further development of the measurement protocol to date high-dose natural samples.

Keywords: Violet Stimulated Luminescence, VSL, Dating, Quartz, MAAD.

1. INTRODUCTION

Optically stimulated luminescence (OSL) is a trapped-charge technique used to date the last exposure to sunlight of mineral grains contained in sedimentary deposits, primarily quartz and potassium feldspar (Aitken, 1985, 1998; Huntley *et al.*, 1985). The technique is of significant relevance to date Quaternary sequences and

archaeological contexts, given the ubiquity of these minerals on Earth's surface deposits and its dating range surpassing the radiocarbon dating limit (~50 ka).

Conventionally, the measurement of quartz OSL is made by stimulating the sample with blue light (hereafter "BSL" for Blue Stimulated Luminescence) and detecting the emitted luminescence in the ultra-violet range (Aitken, 1998). In the laboratory, the amount of energy stored in the mineral is measured as a dose (Gy); the rate of absorption of energy (dose rate, Gy/ka) is derived from

Corresponding author: M. Sontag-González
e-mail: msg493@uowmail.edu.au

knowledge of the natural radioactivity in the sediment. The quotient of these two values (dose/dose rate) gives the burial time (time since deposition). With the accumulation of dose, the luminescence signal increases as the OSL sensitive electron traps fill, reaching a saturation level at ~100–250 Gy (Jain, 2009; Wintle and Adamiec 2017), constraining the maximum time for which BSL dating is applicable to around 100–250 ka, considering a low dose rate of 1 Gy/ka.

Violet Stimulated Luminescence (VSL), first introduced by Jain (2009), is believed to access charges from a deep trap with an extended dose-response saturation in the kGy range. Known age samples with natural doses smaller than 200 Gy have been successfully dated with VSL using single aliquot regenerative dose (SAR) protocols (Murray and Wintle, 2000; Ankjærgaard *et al.*, 2013; Porat *et al.*, 2018). However, older samples show SAR-derived age underestimation of up to 80% (Ankjærgaard *et al.*, 2015, 2016; Colarossi *et al.*, 2018; Morthekai *et al.*, 2015). SAR protocols are in general preferred for OSL dating (Wintle and Murray, 2006), but differences in signal decay and sensitivity changes between the natural and regenerative doses suggest that this approach may be inapplicable to the VSL signal at high doses (>200 Gy; Ankjærgaard *et al.*, 2015, 2016; Colarossi *et al.*, 2018). In order to overcome these drawbacks, Ankjærgaard *et al.* (2016) suggested the use of a multiple aliquot additive dose (MAAD) protocol to build a dose-response curve (DRC). Here we aim to assess the performance of the two approaches on known age archaeological sediment samples with doses ranging ~70–900 Gy.

2. SITES AND SAMPLES DESCRIPTION

For our investigation, we selected four sediment samples of known ages, based on their varied expected equivalent doses (D_e), as follows (Table 1):

- Sample X6717 (Grotte Mandrin, France) is from Level B2 (cultural attribution Proto-Aurignacian; Slimak, 2008) and has an OSL D_e of 67.3 ± 3.0 Gy determined by conventional BSL-SAR measurements, using a preheat/cut heat combination of 240/200°C.
- Sample X6889 (Sima de las Palomas, Spain) is from the eastern wall in sector SEXT and has a D_e of 204.5 ± 16.3 Gy, determined by conventional BSL-SAR using a preheat/cut heat combination of 260/220°C. An age of 102.1 ± 12.0 ka for this sample is in agreement with U-series dating at the site (Walker *et al.*, 2012, 2017).
- Sample X6444 is from the sandy deposits of the extinct Bytham/Baginton Pleistocene fluvial system at Brooksby Quarry (UK), originating from a layer of preserved bedding >30 cm thick. Sediment ESR dates for the sand and gravels unit at this site place it at 300–400 ka, but are believed to be underestimated based on lithostratigraphy (Voinchet *et al.*, 2015). In

general, there is still debate over which glaciation event preceded this fluvial system, either in MIS 6 or before MIS 12 (Gibbard *et al.*, 2013), so that a conservative minimum age of ~200 ka is expected for this sample, corresponding to a dose >300 Gy.

- Sample X6888 (Cueva Negra, Spain) is from layer 4v of the southern wall and is ~50 cm above the layer with evidence of fire (see Angelucci *et al.* (2013) for the site's stratigraphy). According to the biostratigraphy (Jiménez *et al.*, 2018) and palaeomagnetism (Scott and Gibert, 2009) of the site, an age of 780–990 ka has been determined for this sample, corresponding to an expected D_e range of 600–1190 Gy.

Table 1. Details of the studied samples.

Site	Sample code	Dating method	Age (ka)	Expected dose (Gy)
Grotte Mandrin, France	X6717	BSL	41 ± 3	67.3 ± 3.0
Sima de las Palomas, Spain	X6889	BSL	102.1 ± 12.0	204.5 ± 16.3
Brooksby Quarry, UK	X6444	geology	>200	>300
Cueva Negra, Spain	X6888	palaeomagnetism, biostratigraphy	780–990	600–1190

3. METHODS

Sample pretreatment

Sample X6717 was collected under opaque tarps and with dim orange lighting, and all other samples were collected in light-safe tubes hammered into profile walls. All samples were opened under subdued amber light in the luminescence dating laboratory of the Research Laboratory for Archaeology and History of Art in Oxford, UK. After wet-sieving, the 90–250 or 180–255 μm size fraction received chemical treatment with HCl (10%) to remove carbonates and with concentrated HF (40%) to remove feldspar contamination and alpha-irradiated layers. Sample X6717 received an additional density separation step (sodium polytungstate at a density of 2.62 g/ml) prior to HF etching.

Procedures

The luminescence measurements were conducted on a *lexsyg* research system (Freiberg Instruments GmbH) (Richter *et al.*, 2013). Aliquots were stimulated with blue (458 nm) or violet (405 nm) light on continuous wavelength mode with 90% of the maximum power of 100 mW/cm². Emitted luminescence was filtered through Hoya U340 (2.5 mm) and AHF Brightline 340/26 (5 mm) filters prior to measurement. Artificial irradiation was

conducted using a $^{90}\text{Sr}/\text{Y}$ annular source of beta radiation. Single aliquots each containing hundreds of grains were prepared using stainless steel cups, as we found that they yielded lower background than aluminium cups.

4. SAR PROTOCOL

We used the post-blue (pB) VSL-SAR protocol of Hernandez and Mercier (2015), where the preheating step is fixed at 260°C for 10 s (Table 2). All samples displayed similar behaviour, except for X6889, which didn't display a VSL signal. Examples of decay curves for the three samples displaying the expected signal decay shape using the SAR protocol are shown in Fig. 1A, 1D, 1G (each row corresponds to one sample). The intensity of the VSL signal is around 100 times lower than the BSL signal (Fig. 1, insets). Moreover, the VSL signal reaches a background level after ~300 s, while the BSL signal reaches a background level in ~2 s.

Dose-response curves were built for samples X6717, X6444 and X6888. The VSL signal was integrated over the first 300 s signal interval and taking the 400–500 s interval as background, while the BSL signal was integrated using the first 0.09 s of signal and the last 10 s as background. Fig. 1B, 1E, 1H show the VSL and BSL growth of the sensitivity-corrected signal (L_x/T_x) of representative aliquots for the three samples fitted with a double saturation exponential function. Equivalent dose (D_e) values were obtained by interpolation of L_n/T_n onto this function (Duller, 2015; Peng *et al.*, 2013). Between three and thirteen aliquots of each sample were analysed in this manner, though a few were fitted with an exponential plus linear function.

It has been reported that variation of the VSL signal integration limits affects the D_e estimate, because of the contribution from different components. Ankjærgaard *et al.* (2013) defined two components, A and B (0–3 and 9–29 s, respectively), using an early-background approach (3–10 and 29–80 s, respectively). A longer signal interval (0–300 s, 400–500 s BG) has been suggested by

Hernandez and Mercier (2015) to account for differences in decay shape. To investigate the effect of integration limits, D_e values were determined using the three integration intervals mentioned above and a late-background fast interval (0–0.09 s; 450–500 s BG) (Fig. 1C, 1F, 1I). Average D_e values were calculated using the central age model (CAM) (Burow, 2017; Galbraith *et al.*, 1999). Aliquots were accepted if the following criteria were met: natural test dose signal (T_n) at least 3σ above the corresponding background and with a relative error under 25%, negligible recuperation (<5%) and recycling ratio consistent with unity (1.0 ± 0.1). The laser power used in this study was similar to that in Ankjærgaard *et al.* (2013), so we have maintained the original interval lengths, though it should be noted that our decays are expected to occur ~20% faster. The laser power used by Hernandez and Mercier (2015) was almost 4x higher than in the present study; however, we used the same integration limit of 0–300 s, seen as the aim of this interval is not to capture a single component, but rather to capture any changes in decay curve shape by integrating over a long decay time.

Use of the different intervals resulted in a variation in CAM D_e values and in the number of accepted aliquots (Table 3). For the youngest sample (X6717), the component B interval (9–29 s) CAM D_e of 69.8 ± 11.8 Gy best agreed with the expected result of 67.3 ± 3.0 Gy. For the two older samples (X6444 and X6888), the determined D_e were mostly below the expected dose, except for that of component B (9–29 s) for X6444, 339.9 ± 67.4 Gy, expected to be >300 Gy. The other intervals for X6444 delivered D_e below the minimum expected dose by 25–50%. The CAM D_e values of X6888 underestimated the expected dose range of 600–1190 Gy for this sample by 60–75%, depending on the signal interval used. For all samples, component B resulted in the highest dose equivalents. It is noteworthy that component B has previously been considered unsuitable for dating due to high recuperation rates up to ~20% (Morthekai *et al.*, 2015) and larger underestimations than component A (Ankjærgaard *et al.*, 2013).

Table 2. Protocols used in this study. Alterations are in bold. Note that for the MAAD protocol, only the measurement parameters were based on Ankjærgaard *et al.* (2016), not the method to estimate the D_e .

Step	SAR (adapted from Hernandez and Mercier (2015))	MAAD (adapted from Ankjærgaard <i>et al.</i> (2016))	Function
0	-	Additive dose	
1	Preheat (260°C, 10 s)	Preheat (300°C, 100 s or 10 s)	Empty thermally unstable components
2	Blue bleach (125°C, 40 s)	Blue bleach (125°C, 100 s)	Empty shallow trapped charge
3	VSL (125°C, 500 s)	VSL (30°C, 500 s)	Measure deep trapped charge (L_n , L_x or L_a)
4	Violet bleach (200°C, 500 s)	-	Reduce recuperation
5	Test dose (18 Gy)	Test dose (50 Gy)	Sensitivity correction
6	Preheat (260°C, 10 s)	Preheat (300°C, 100 s or 10 s)	Empty thermally unstable components
7	Blue bleach (125°C, 40 s)	Blue bleach (125°C, 100 s)	Empty shallow trapped charge
8	VSL (125°C, 500 s)	VSL (30°C, 500 s)	Measure deep trapped charge (T_n , T_x or T_a)
9	Violet bleach (200°C, 500 s)	-	Reduce recuperation
10	Regenerative dose	-	

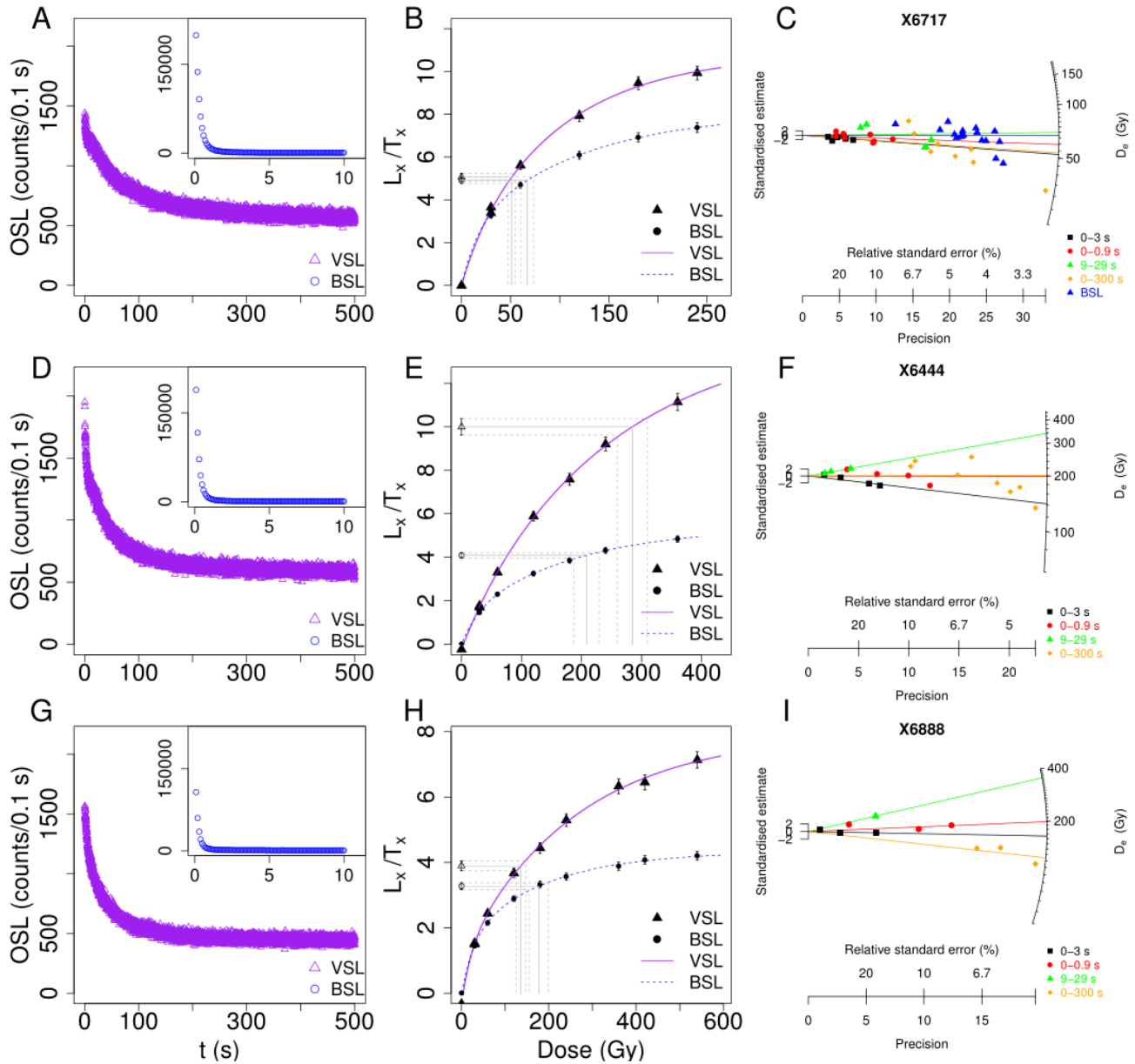


Fig. 1. SAR protocol results for samples X6717 (A,B,C), X6444 (D,E,F) and X6888 (G,H,I). (A,D,G) display the natural signal decay curves, with purple triangles representing the VSL signal and insets showing the preceding BSL (blue circles) for comparison. (B,E,H) show the dose response using the long signal interval (0–300 s; 400–500 s BG) of VSL (triangles) and fast interval (0–0.9 s; 90–100 s BG) of BSL (circles). Error bars show standard errors. (C,F,I) show the D_e distributions of four VSL signal intervals: 0–3 s (BG: 3–10.5 s) (black squares), 0–0.9 s (BG: 450–500 s) (red circles), 9–29 s (BG: 29–80 s) (green triangles) and 0–300 s (BG: 400–500s) (orange diamonds). The BSL D_e values of X6717 (blue triangles) are shown for comparison. Lines show the CAM D_e of each interval. Radial plots modified from Dietze and Kreutzer (2017) (R Core Team, 2016).

It is also of note that for all samples the VSL growth curve saturates earlier than expected, with $2D_0$ values in the range 350–600 Gy. This is in sharp contrast to the dose-response reported previously (Ankjærgaard *et al.*, 2013, 2016), where the VSL signal has been shown to saturate at doses over 2000 Gy. This indicates that the targeted late-saturating VSL signal was not well isolated for our samples with this protocol.

5. MAAD PROTOCOL

Ankjærgaard *et al.* (2016) reported a difference in shape between the natural and the subsequent regenerative dose VSL decay curves, which can induce discrepancy in the D_e estimates. These authors suggested the use of a MAAD protocol in order to circumvent this issue. Here, we applied a post-blue VSL MAAD protocol following

Table 3. VSL D_e estimates using the SAR protocol. The VSL D_e values that match the expected dose at 1 sigma are in bold type.

Sample	Signal (s)	Background (s)	# ¹	Overdispersion (%)	$D_e \pm se$ (Gy) ²
X6717	0–0.9	450–500	8/12	13.3 ± 6.5	59.7 ± 4.1
	0–300	400–500	10/12	32.1 ± 7.4	53.6 ± 5.5
	0–3	3–10.5	7/12	-	52.4 ± 3.9
	9–29	29–80	5/12	36.7 ± 12.3	69.8 ± 11.8
X6444	0–0.9	450–500	4/13	14.7 ± 8.9	199.4 ± 19.8
	0–300	400–500	8/13	27.2 ± 7.2	202.2 ± 20.1
	0–3	3–10.5	4/13	-	141.5 ± 14.1
	9–29	29–80	3/13	-	339.9 ± 67.4
X6888	0–0.9	450–500	3/3	-	199.0 ± 12.4
	0–300	400–500	3/3	5.5 ± 4.8	124.7 ± 5.8
	0–3	3–10.5	3/3	-	165.2 ± 25.2
	9–29	29–80	1/3	-	354.5 ± 61.0

¹ number of accepted/measured aliquots² D_e values were determined using the Central Age Model

the parameters in Ankjærgaard *et al.* (2016), where the VSL signal is detected after a high temperature preheat of 300°C for 100 s. In initial measurements, we observed a significant depletion of the VSL signal (Fig. 2A, orange triangles). Therefore, we shortened the preheat length to 10 s. Details of the protocol are reported in Table 2. Series of three and six aliquots were used for each dose point of sample X6444 (0, 100, 200, 400 Gy) and X6889 (0, 50, 100, 200, 400 Gy), respectively. Aliquots were accepted if the natural test dose signal (T_n) was at least 3σ above the corresponding background and had a relative error under 25%. Outliers were rejected if the normalised median absolute deviation (nMAD) of $\log L_a/T_a$ of each dose point was greater than 2.5 (using 1.4826 as the correction factor for a normal distribution) (Powell *et al.*, 2002, Clarkson *et al.*, 2017) and from the accepted data a CAM was calculated for each dose point (Galbraith *et al.*, 1999). D_e values were obtained using a classical MAAD approach (Aitken, 1998) by extrapolating the growth curve fitted to the CAM values to 0 dose, since no modern samples were collected at the selected sites.

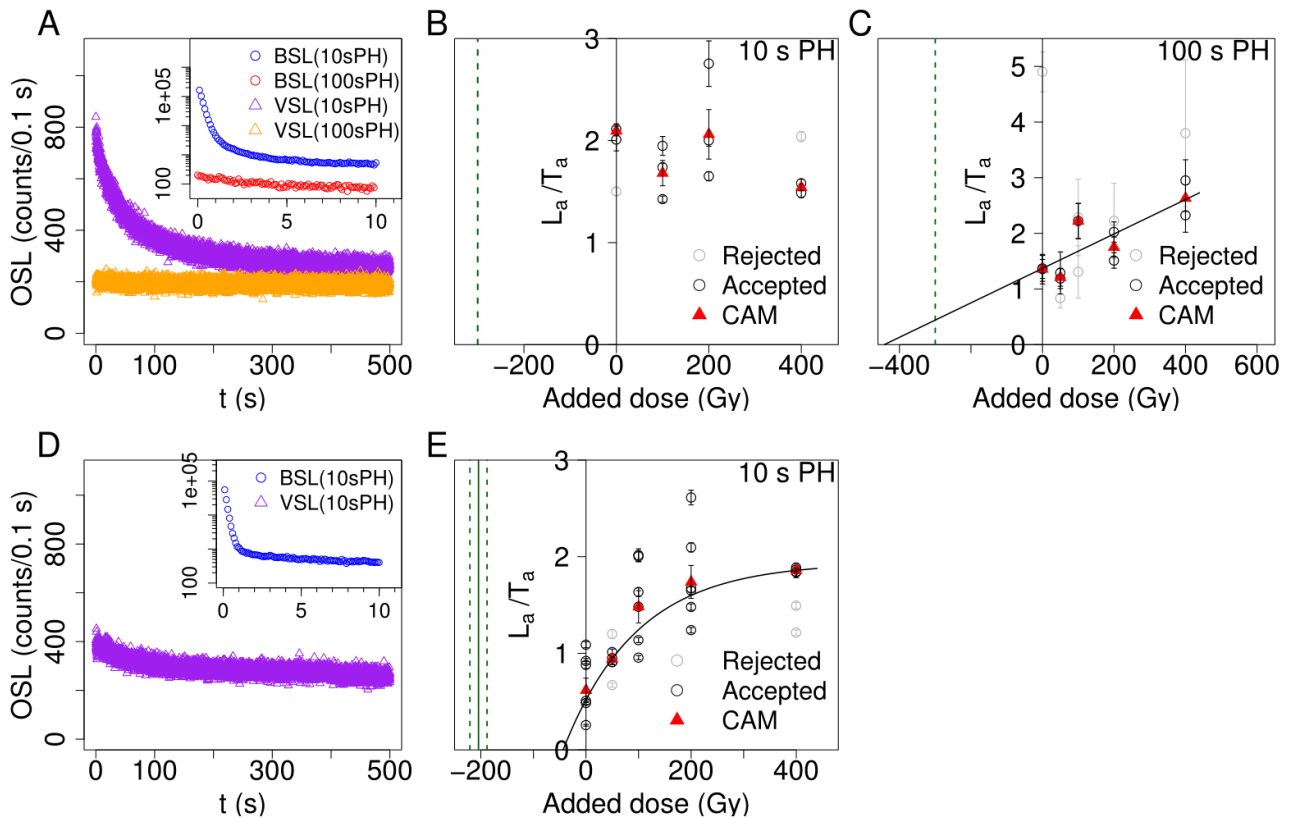


Fig. 2. MAAD protocol results for samples X6444 (A–C) and X6889 (D–E). (A,D) show the natural dose decay curves and (B,C,E) show the dose response using the signal interval 0–300 s (BG: 400–500s). (B,E) resulted from the shortened preheat (10 s) measurement (purple triangles in (A,D)), while (C) resulted from the 100 s preheat measurement (orange triangle in (A)). The CAM of nMAD accepted aliquots were fitted with a linear function in (C) and an exponential function in (E). The green vertical lines correspond to the expected D_e . Error bars show the standard errors.

Fig. 2 shows the MAAD results of samples X6444 and X6889. The VSL decays (**Fig. 2A, 2D**) are similar to those described for the SAR protocol, though the signals are dimmer in this case. An increase of 40°C in preheat temperature (equal lengths of 10 s) led to a 60% initial signal decrease for sample X6444 (cf. **Fig. 1D** and **Fig. 2A**, purple triangles), whereas an increase from 10 to 100 s preheat length (equal temperatures of 300°C) almost fully depleted the signal of this sample (cf. **Fig. 2A** purple and orange triangles). Furthermore, the short preheat of 10 s already significantly depleted the signal of sample X6889 (**Fig. 2D**).

Three different integration intervals were tested to construct a DRC: 0–300 s with a late background, 0–3 s with an early background, and 9–29 s with an early background, with the latter two corresponding to components A and B of Ankjærgaard *et al.* (2013), respectively. None of the three intervals tested for sample X6444 using the shorter preheat length (10 s) displays a clear signal growth with increasing dose, as shown for the 0–300 s interval in **Fig. 2B**. Of the three signal intervals tested for sample X6889 using the 10 s preheat length, only the long signal interval (0–300 s) (**Fig. 2E**) shows a satisfactory dose response. An exponential function was fitted to the CAM of accepted dose points using a Nelder-Mead Simplex algorithm and the absolute value of its intersection with the x-axis, considering its associated uncertainty provides an estimate of the D_e of 43.6 ± 17.6 Gy. When compared with the expected D_e of 204.5 ± 16.3 Gy, we observe an underestimation of around 70%. Additionally, this signal component appears to reach saturation earlier than expected for the VSL signal, with a D_0 value of 140 Gy added dose (atop 204.5 ± 16.3 Gy natural dose), corresponding to a $2D_0$ value of ~ 690 Gy in this case.

Despite the very low VSL signal decay of sample X6444 using the long preheat of 100 s (see **Fig. 2A**), integration of the 0–300 s interval displays a signal growth with increasing added dose (**Fig. 2C**). The best fit of the CAM values was given by a linear function, though the fit is poor, having an adjusted R^2 value of 0.57. Extrapolation of the linear function, considering its residual standard error, delivers a D_e estimate of 442.5 ± 171.3 Gy, which exceeds the minimum expected dose of 300 Gy. Given the poor fit, this result is not deemed significant in terms of age estimation, but the comparison of the signals using the different preheat lengths suggests that the cause of the observed lack of signal growth after the short preheat lies in the dimness of the pB-VSL signal relative to the incompletely bleached slow blue signal.

6. DISCUSSION

We tested the applicability of two protocols, namely a SAR protocol (following Hernandez and Mercier (2015)) and a MAAD protocol (following protocol parameters of Ankjærgaard *et al.* (2016)), to determine the D_e of sedi-

mentary quartz samples using VSL. For one low-dose sample (X6717), the VSL-SAR D_e is in agreement with the expected D_e value of 67.3 ± 3.0 Gy using the component B interval (9–29 s). However, for two higher-dose samples, VSL-SAR resulted in underestimations. The minimum expected D_e of X6444 was only achieved by component B (9–29 s; 339.9 ± 67.4 Gy), while the other intervals underestimated by up to 50%. All signal intervals of X6888 underestimated the expected minimum D_e of 600 Gy by 40–80%. This finding is in agreement with previous research on VSL-SAR, which shows agreement with independent age controls for samples below 200 Gy (Ankjærgaard *et al.*, 2015; Porat *et al.*, 2018), but with severe underestimations of up to 80% reported for samples with expected D_e values of 300–8000 Gy (Ankjærgaard *et al.*, 2015, 2016; Colarossi *et al.*, 2018; Morthekai *et al.*, 2015). For this reason, a MAAD protocol was tested for the higher-dose samples.

The results using the MAAD protocol were more difficult to interpret. Using the short preheat of 10 s, which depletes less of the pB-VSL signal (see **Fig. 2A**), a D_e estimation was only possible using a long integration limit for one of the samples (X6889, **Fig. 2E**), but which underestimated the expected dose of 204.5 ± 16.3 Gy by 70%. It was not possible to build a MAAD growth curve for the other sample (X6444) using this preheat length. The successful growth curve (X6889, **Fig. 2E**) suggests the onset of saturation of the VSL signal already at 700 Gy using the short-preheat MAAD protocol ($2D_0$ value of 690 Gy). This is higher than the saturation observed for the SAR protocol ($2D_0$ range: 350–600 Gy), which had shorter BSL bleach lengths and lower temperature preheats. While the observed MAAD saturation dose would be an improvement relative to conventional BSL dating, it is much lower than the expected value for the VSL signal, which has been shown to grow up to at least 1800 Gy (Ankjærgaard *et al.*, 2016), indicating that the high-dose saturating VSL signal was not successfully isolated in our protocol. This is presumably caused by insufficient bleaching of the slow-blue component. In contrast, using the original 100 s preheat length allowed for a DRC to be constructed, despite the very dim signal. For either preheat lengths, only the long signal integration interval (0–300 s) resulted in growth curves, presumably because the large uncertainty caused by the low signal levels is counterbalanced by the long average.

The signal decay of X6444 using the short preheat (**Fig. 2A**) appears to be dominated by the incompletely bleached slow blue component. One of the slow blue components (S_2 in Singarayer and Bailey (2003) and S_3 in Jain *et al.*, 2003) has been shown to saturate early at 150 Gy (Singarayer and Bailey, 2003), which would explain why we do not observe any signal growth after adding dose atop the natural dose of at least 300 Gy. The early saturation of X6889 can also be explained by an incompletely bleached slow blue component, given that the VSL signal is so dim that any small residual slow

blue would contribute to the signal. Other multiple aliquot approaches may be able to elucidate this issue. For example, in the MAAD protocol of Ankjærgaard *et al.* (2016), the DRC was built using younger samples from the same site, allowing the DRC to be established for low doses even when dating high dose samples. In this case, early signal saturation would be clearly identifiable.

The poor bleaching of the slow blue component in both the SAR and MAAD protocols is probably caused by inappropriate preheating and/or BSL bleach length. Previously, it has been shown that preheat stringency must be balanced between minimizing the slow blue component without excessively depleting the VSL signal. For example, Porat *et al.* (2018) report a doubling of the D_0 value with a 10°C preheat/cutheat increase, but with severe signal depletion. Our results show a similar trend: regardless of signal interval, the MAAD results do not display the expected late-saturating dose response unless the preheat stringency is increased to the point of almost fully depleting the pB-VSL signal, which then leads to large uncertainty. Thus, it seems likely that the pB-VSL of samples X6444 and X6889 are too dim relative to the slow blue component to be measurable with the present experimental set-up.

More work is needed to optimise protocol parameters that isolate the late-saturating pB-VSL, for which brighter samples should be chosen. It must also be investigated what the relationship between the slow blue component and the pB-VSL signal is and whether there is a correlation in the brightness of the components. Our results using the long preheat indicate that it may be possible to date dim samples for which almost no signal decay is observed, but that a much larger number of aliquots would be needed to statistically counter the large scatter caused by the low signal brightness.

7. CONCLUSION

Our findings indicate the need for further refinement of the VSL protocol to make it suitable to date natural high-dose samples. In particular, the sufficient bleaching of the slow blue component without depletion of the pB-VSL signal seems to be problematic. The behaviour of VSL also appears to be sample-dependent, which may make it challenging to establish a broadly-applicable protocol.

ACKNOWLEDGEMENTS

Michael Walker is thanked for access to Cueva Negra and Sima de las Palomas sites, Ludovic Slimak to Grotte Mandrin (sample collected under the ERC Palaeochron project) and University of Leicester Archaeological Services to Brooksby Quarry. David Peat is thanked for laboratory assistance and Laine Clark-Balzan for help in the dose rate analysis. Xue Rui is thanked for revising the manuscript. Part of this study was presented at the UK

Luminescence and ESR Dating Meeting 2016. B.L. is supported by an Australian Research Council Future Fellowship (FT140100384). M.S.-G. is supported by a UOW international postgraduate tuition award and a Future Fellow PhD scholarship. The authors are thankful for the constructive comments of an anonymous reviewer.

REFERENCES

- Aitken MJ, 1985. *Thermoluminescence dating*. Academic Press, London.
- Aitken MJ, 1998. *An Introduction to Optical Dating*. Oxford University Press, Oxford.
- Angelucci D, Anesin D, López-Martínez M, Haber-Urriarte M, Rodríguez-Estrella T and Walker MJ, 2013. Rethinking stratigraphy and site formation of the Pleistocene deposit at Cueva Negra del Estrecho del Río Quipar (Caravaca de la Cruz, Spain). *Quaternary Science Reviews* 80: 195–199. DOI 10.1016/j.quascirev.2013.09.009.
- Ankjærgaard C, Guralnik B, Buylaert J-P, Reimann T, Yi SW and Wallinga J, 2016. Violet stimulated luminescence dating of quartz from Luochuan (Chinese loess plateau): Agreement with independent chronology up to ~ 600 ka. *Quaternary Geochronology* 34: 33–46, DOI 10.1016/j.quageo.2016.03.001.
- Ankjærgaard C, Guralnik B, Porat N, Heimann A, Jain M and Wallinga J, 2015. Violet stimulated luminescence: geo- or thermochronometer? *Radiation Measurements* 81: 78–84, DOI 10.1016/j.radmeas.2015.01.011.
- Ankjærgaard C, Jain M and Wallinga J, 2013. Towards dating Quaternary sediments using the quartz Violet Stimulated Luminescence (VSL) signal. *Quaternary Geochronology* 18: 99–109, DOI 10.1016/j.quageo.2013.06.001.
- Burow C, 2017. calc CentralDose(): Apply the central age model (CAM) after Galbraith *et al.* (1999) to a given De distribution. Function version 1.3.2. In: Kreutzer S, Dietze M, Burow C, Fuchs MC, Schmidt C, Fischer M, Friedrich, J. (2017). *Luminescence: Comprehensive Luminescence Dating Data Analysis*. R package version 0.7.4. <https://CRAN.R-project.org/package=Luminescence>
- Clarkson C, Jacobs Z, Marwick B, Fullagar R, Wallis L, Smith M, Roberts RG, Hayes E, Lowe K, Carah X, Florin SA, Mcneil J, Cox D, Arnold LJ, Hua Q, Huntley J, Brand HEA, Manne T, Fairbairn A, Shulmeister J, Lyle L, Salinas M, Page M, Connell K, Park G, Norman K, Murphy T and Pardoe C, 2017. Human occupation of northern Australia by 65,000 years ago. *Nature* 547: 306–310, DOI 10.1038/nature22968.
- Colarossi D, Chapot MS, Duller GA and Roberts HM, 2018. Testing single aliquot regenerative dose (SAR) protocols for violet stimulated luminescence. *Radiation Measurements* 120: 104–109, DOI 10.1016/j.radmeas.2018.02.005.
- Dietze M and Kreutzer S, 2017. plot RadialPlot(): Function to create a Radial Plot. Function version 0.5.3. In: Kreutzer S, Dietze M, Burow C, Fuchs MC, Schmidt C, Fischer M and Friedrich J, 2017. *Luminescence: Comprehensive Luminescence Dating Data Analysis*. R package version 0.7.4. URL <https://CRAN.R-project.org/package=Luminescence>
- Duller GAT, 2015. The Analyst software package for luminescence data: overview and recent improvements. *Ancient TL* 33: 1–8.
- Galbraith RF, Roberts RG, Laslett GM, Yoshida H and Olley JM, 1999. Optical dating of single and multiple grains of quartz from Jinmium rock shelter, Northern Australia: Part I, Experimental design and statistical models. *Archaeometry* 41: 339–364, DOI 10.1111/j.1475-4754.1999.tb00987.x.
- Gibbard PL, Turner C and West RG, 2013. The Bytham river reconsidered. *Quaternary International* 292: 15–32, DOI 10.1016/j.quaint.2012.08.2053.
- Hernandez M and Mercier N, 2015. Characteristics of the post-blue VSL signal from sedimentary quartz. *Radiation Measurements* 78: 1–8, DOI 10.1016/j.radmeas.2015.05.001.

- Huntley DJ, Godfrey-Smith DI and Thewalt MLW, 1985. Optical dating of sediments. *Nature* 313: 105–107, DOI 10.1038/313105a0.
- Jain M, 2009. Extending the dose range: Probing deep traps in quartz with 3.06 eV photons. *Radiation Measurements* 44: 445–452, DOI 10.1016/j.radmeas.2009.03.011.
- Jain M, Murray AS and Bøtter-Jensen L, 2003. Characterisation of blue-light stimulated luminescence components in different quartz samples: implications for dose measurement. *Radiation Measurements* 37: 441–449, DOI 10.1016/S1350-4487(03)00052-0.
- Jiménez AL, Haber-Urriarte M, López-Martínez M and Walker MJ, 2018. Small-mammal indicators of biochronology at Cueva Negra del Estrecho del Río Quípar (Caravaca de la Cruz, Murcia, SE Spain). *Historical Biology*, DOI 10.1080/08912963.2018.1462804.
- Morthekai P, Chauhan PR, Jain M, Shukla AD, Rajapara HM, Krishnan K, Sant DA, Patnaik R, Reddy DV and Singhvi AK, 2015. Thermally re-distributed IRSL (RD-IRSL): A new possibility of dating sediments near B/M boundary. *Quaternary Geochronology* 30: 154–160, DOI 10.1016/j.quageo.2015.05.018.
- Murray AS and Wintle AG, 2000. Luminescence dating of quartz using an improved single-aliquot regenerative-dose protocol. *Radiation Measurements* 32: 57–73, DOI 10.1016/S1350-4487(99)00253-X.
- Peng J, Dong Z, Han F, Long H and Liu X, 2013. R package numOSL: numeric routines for optically stimulated luminescence dating. *Ancient TL* 31: 41–48.
- Porat N, Jain M, Ronen A and Horwitz LK, 2018. A contribution to late Middle Paleolithic chronology of the Levant: New luminescence ages for the Atlit Railway Bridge site, Coastal Plain, Israel. *Quaternary International* 464: 32–42, DOI 10.1016/j.quaint.2017.06.017.
- Powell R, Hergt J and Woodhead J, 2002. Improving isochron calculations with robust statistics and the bootstrap. *Chemical Geology* 185: 191–204, DOI 10.1016/S0009-2541(01)00403-X.
- R Core Team, 2016. *R: a language and environment for statistical computing*. Vienna, Austria. <https://www.r-project.org/>.
- Richter D, Richter A and Dornich K, 2013. LEXSYG a new system for luminescence research. *Geochronometria* 40: 220–228, DOI 10.2478/s13386-013-0110-0.
- Scott GR and Gibert L, 2009. The oldest hand-axes in Europe. *Nature* 461: 82–85, DOI 10.1038/nature08214.
- Singarayer JS and Bailey RM, 2003. Further investigations of the quartz optically stimulated luminescence components using linear modulation. *Radiation Measurements* 37: 451–458, DOI 10.1016/S1350-4487(03)00062-3.
- Slimak L, 2008. The Neronian and the historical structure of cultural shifts from Middle to Upper Palaeolithic in Mediterranean France. *Journal of Archaeological Science* 35: 2204–2214, DOI 10.1016/j.jas.2008.02.005.
- Voinchet P, Moreno D, Bahain J, Tissoux H, Tombret O, Falguères C, Moncel M, Schreve D, Candy I, Antoine P, Ashton N, Beamish M, Cliquet D, Despriée J, Lewis S, Limondin-Lozouet N, Loch J, Parfitt S and Pope M, 2015. New chronological data (ESR and ESR/U-series) for the earliest Acheulian sites of north-western Europe. *Journal of Quaternary Science* 30: 610–622, DOI 10.1002/jqs.2814.
- Walker MJ, López-Martínez MV, Ortega-Rodríguez J, Haber-Urriarte M, López-Jiménez A, Avilés-Fernández A, Polo-Camacho JL, Campillo-Boj M, García-Torres J, García JSC, del Toro MSN and Rodríguez-Estrella T, 2012. The excavation of buried articulated Neanderthal skeletons at Sima de las Palomas (Murcia, SE Spain). *Quaternary International* 259: 7–21, DOI 10.1016/j.quaint.2011.03.034.
- Walker MJ, Sontag-González M, Haber-Urriarte M, López-Martínez M, Black S and Schwenninger J-L, 2017. Preliminary dating of deep layers at Sima de las Palomas del Cabezo Gordo (Torre Pacheco, Murcia, Spain). *Proceedings of the European Society for the Study of Human Evolution* 6, 210. https://www.eshe.eu/static/eshe/files/PESHE/PESHE_2017_FINALE.pdf
- Wintle AG and Adamiec G, 2017. Optically stimulated luminescence signals from quartz: A review. *Radiation Measurements* 98: 10–33, DOI 10.1016/j.radmeas.2017.02.003.
- Wintle AG and Murray AS, 2006. A review of quartz optically stimulated luminescence characteristics and their relevance in single-aliquot regeneration dating protocols. *Radiation Measurements* 41: 369–391, DOI 10.1016/j.radmeas.2005.11.001.